

# IMPROVEMENTS IN TWO-STEP MODEL OF HYDROGEN DETONATIVE COMBUSTION: MODEL DESCRIPTION AND SENSITIVITY TO ITS PARAMETERS

Zaev I.A.<sup>1</sup>, Kirillov I.A.<sup>2</sup>

<sup>1</sup>RRC “Kurchatov institute”, 1 Kurchatov Sq., Moscow, 123182, Russia, [i\\_zaev@mail.ru](mailto:i_zaev@mail.ru)

<sup>2</sup>RRC “Kurchatov institute”, 1 Kurchatov Sq., Moscow, 123182, Russia, [kia@hepti.kiae.ru](mailto:kia@hepti.kiae.ru)

## ABSTRACT

In the present paper the two-stage model of detonative combustion of hydrogen is presented. The following improvements are described: accurate description of the heat release stage of combustion; the clear physics-based procedure for calculation of the parameters of the proposed model; sample calculations of the detonation wave in hydrogen/air mixtures in wide range of conditions, showing that the proposed model performs well in a wide range of conditions (pressures, temperatures, mixture compositions). The results of the 2D simulations of the detonation cell are presented for the hydrogen/oxygen/argon mixture as example to show the performance and accuracy of the model, presented in this paper.

## 1 INTRODUCTION

During the past decade the worldwide attention in the combustion community was paid to hydrogen global energy as an alternative to traditional energy and fuels (petroleum, natural gas, etc.). Research and development in this area is impossible without numerical experiment, especially CFD (computational fluid dynamics), which helps to understand deeper the physics and to quantitatively estimate the consequences of the accidents with the hydrogen leakage and explosions.

In hydrogen safety most of the problems are related with confined reactive systems with complex multidimensional geometry. Practical multidimensional CFD simulations using detailed kinetic schemes are extremely time-consuming and can be made only for decisive runs. Hence, the robust and accurate models for chemistry of the hydrogen combustion are necessary.

Since the 1960-th several approaches to simulate the chemical reactions in blast and detonation waves have been proposed:

- 1) *Arrhenius one-step kinetics*. The first model, which was used for simulation of detonations, is the simple one-step reaction with rate, depending on temperature according to Arrhenius law [1]. Though this model is extensively used in theoretical studies of detonation, it is known that it hardly can reproduce self-ignition and combustion properties of the real fuels, as for most of the reactive mixtures the combustion proceeds in two stages – induction and heat release, which has independent time scales, but this is not the case for the simple one-step reaction.
- 2) *Induction parameter models (IPM model, two-step model)*. To overcome this deficiency of the single-step reaction model, the Induction Parameter Model (IPM) was introduced by Korobeinikov in 70s [2] to simulate the explosions in gases.

This model is based on the notion, that combustion of the fuels in air is a chain-branching process, which is characterised by two successive stages. During the first, induction, stage the active intermediate species are accumulated. Usually this stage is thermo-neutral or slightly endothermic. When the amount of active intermediate species becomes large, they begin to react with the release of the heat and the second, heat release, stage begins. The duration of these stages is characterized by an independent time scales referred to as induction time  $t_i$  and heat release time  $t_{hr}$ .

The different modifications of this model were extensively used to simulate the explosions and multidimensional detonations in gases [3 – 7]. For example, Sichel proposes the modification of the IPM model, where the equilibrium composition of the reactive mixture in the C-J state is used to calculate correct speed of the detonation wave without necessity to introduce the reverse reaction. Alternative formulation of the IPM model was proposed by Nikolaev [6], where the molar weight of the reactive mixture is used as parameter, which describes the degree of the conversion from initial mixture composition to products. It is

necessary to note, that the IPM approach is very useful in CFD simulations because of simplicity of its implementation in CFD code and low computational cost.

- 3) *Two-reactions description of the hydrocarbon detonations.* Another approach to reduce the chemical kinetics of the combustion of complex fuels such as hydrocarbons was proposed by B. Varatharajan and F.A. Williams [8]. The main idea of the approach is to reduce the large detailed kinetic mechanism to two reactions using the quasi-steady-state and quasi-equilibrium assumptions. While this approach is promising for CFD simulation, it has several difficult tasks in its implementation:
  - Extensive kinetic analysis is required to establish the limiting stages of the induction stage;
  - In the final version of the approach some empirical fitting parameters are required;
  - In general the parameters of the model (stoichiometric coefficients of the reactions) depend on local flow conditions;
  - The number of species is about 7 – 8 (IPM model has only two parameters).
- 4) *Intrinsic low-dimensional manifolds.* In [9] the ILDM approach was developed for simulation of multidimensional detonations in hydrogen-oxygen mixtures and was validated against the cell sizes of the self-sustaining detonation waves. As it was noted by the author of [9], the ILDM approach fails in the simulation of the induction period of the chemical reactions and research is needed in this direction to make the ILDM approach more flexible for detonation simulations.

In comparison with the approaches [8, 9] the IPM model has several advantages. First, it could reproduce the ignition delay times with the accuracy, comparable with the accuracy of detailed kinetic mechanism without any simplification assumptions. Second, the reaction progress is described with two successive stages and variables, so during the every stage of the combustion the reaction looks like a single variable process and number of variables, stored in the memory of the computer is reduced in comparison with the detailed kinetic mechanism. Third, the simple numerical methods like Runge-Kutta can be applied for integration of the chemical kinetic equations instead of complex stiff ODE solvers.

As it was described above, several versions of the IPM model exists [3 – 7]. The comparative study of these models reveals the following deficiencies or disagreements between the models:

- 1) the heat release rate is described in different way in the model of Sichel [5] and Nikolaev [6], i.e. in [5] the heat release rate does not depend on local pressure/density and the reaction is first order, while in [6] the heat release rate depends on pressure and the reaction is second-order;
- 2) the description of the induction stage is based on the calculation of the portions of the induction time at several conditions from the analytical relations. Unfortunately even in [5] the newly proposed expression does not capture the well known non-monotonous behavior of the ignition delay time on pressure in hydrogen-air or hydrogen oxygen mixtures (according to relation, proposed in [5], the induction time tends to infinity when pressure increases, which is not the case in the simulations with the detailed mechanism);
- 3) in [5] the approach is proposed to account for the real thermo-chemical properties of the reactive mixture by implementing the polynomial dependence of the specific heat on temperature; the calculation of the thermodynamic functions of the combustible mixture contains summation of the polynomial functions over all species of the mixture and can reduce the speed of the simulations, when the number of mixture components is as large as for hydrocarbons (the reduced chemical kinetic mechanism of ethylene combustion [11] contains 21 species) thus resulting into the much more computational operations per time step.

In the present paper we describe the new version of the two-step (IPM) model, developed in the RRC “Kurchatov Institute” for the hydrogen and hydrogen-containing fuels. It is designed specifically to eliminate the disadvantages, listed above.

## 2 HEAT RELEASE IN HYDROGEN DETONATIVE COMBUSTION

The different approaches to the description of the heat release stage in IPM models is probably related with the general notion, that the dynamic detonation parameters (cell size, critical energy of direct detonation initiation, critical diameter of the detonation diffraction) are directly related with induction length of the Zel’dovich-von Neumann-Doering (ZND) detonation structure of the Chapman-Jouguet (CJ) detonation. Therefore the heat release is only additional stage, which should be described in some way to provide transition from reagents to products. As it will be shown in the next sections it is not generally true and the heat release stage of the hydrogen combustion should be

studied more carefully to develop unified description of the heat release and to improve the accuracy of the critical conditions in the detonation phenomena.

The calculation of the heat-release stage parameters is directly related with the heat release time calculation. Therefore, the results of the calculation of the heat release time will be presented first and the model parameters for the heat-release stage will be reported in the next sections.

The following physical model is considered. Homogeneous hydrogen-air (oxygen) mixture is at initial temperature  $T_0$  and initial pressure  $P_0$ , mixture composition is defined by the equivalence ratio of the initial hydrogen and oxygen concentrations  $ER = [H_2]_0/2[O_2]_0$ , self-ignites at constant volume adiabatic condition, reaching the adiabatic temperature after the combustion is completed. The simulations are carried out with the Chemical Workbench<sup>®</sup> integrated environment [10] with the detailed kinetic mechanism [11].

Fig. 1 illustrates the definition of the heat release time  $t_{hr}$  on the basis of the results of the simulations with the detailed chemical kinetic model. Namely, the tangential line is plotted at the inflection point of the curve  $T(t)$ . Its intersection with the level of the initial temperature is time  $t_1$  and its intersection with the level of the temperature of adiabatic combustion at constant volume  $T_{ad}$  is time  $t_2$ . The heat-release time is difference

$$t_{hr} = t_2 - t_1.$$

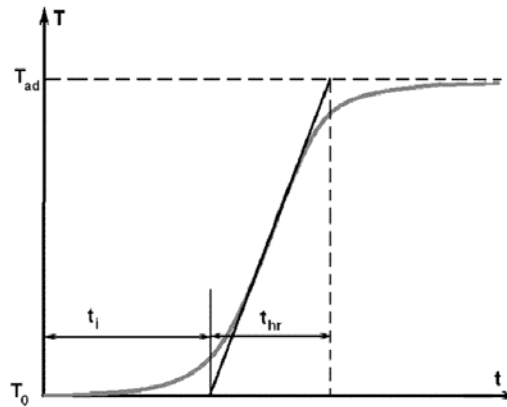


Figure 1. Definition of the heat release time.  $T_0$  – initial temperature,  $T_{ad}$  – adiabatic temperature of combustion at constant volume conditions.

This definition of the heat release time relates two internal parameters of the self-ignition and combustion process: maximum heat release rate (through the slope of the tangential line) and adiabatic temperature of combustion; it does not rely on user-specific input (as is usually for induction time definitions).

The examples of the calculated heat release time at different conditions are presented on Fig. 2. On the Fig. 2a the dependencies of the heat release time on initial temperature of the self-igniting stoichiometric  $H_2$ -air mixture are presented for initial pressures 1 atm and 15 atm. In both cases the dependence on initial temperature is weak and can be described by a power law, e.g. for the initial pressure of 1 atm  $t_{hr} \approx 10^{-7} \cdot T_0^{0.62}$  s (the temperature is given in Kelvins). If the initial pressure increases, the exponent of the power law decreases and for  $P_0 = 15$  atm  $t_{hr} \approx 6 \cdot 10^{-7} \cdot T_0^{-0.165}$  s. Since the heat release time changes on the factor of 1.5 when the initial temperature changes twice, it is useful to assume that the heat release time does not depend on initial temperature and is equal to 10  $\mu$ s at initial pressure 1 atm. On Fig. 2b the dependencies of the heat release time on initial pressure are presented for two initial conditions:  $T_0 = 1200$  K,  $ER = 1$  and  $T_0 = 1500$  K,  $ER = 2$ . Both of the dependencies are the straight lines at the logarithmic scaled representation and the slope of the line is approximately equal to 1.5, i.e.  $t_{hr} \sim P_0^{-1.5}$ .

The following relation can be used for calculation of the heat release time in  $H_2$ -air mixtures in the range of initial conditions  $T_0 = 1100 - 2100$  K and  $P_0 = 1 - 50$  atm

$$t_{hr}(T_0, P_0, ER) = 10^{-5} \cdot \left( \frac{T_0}{1100} \right)^{0.64 - 0.055 \cdot P_0} \cdot P_0^{-1.5} \cdot ER^{-0.6} \text{ s,}$$

the temperature is measured in Kelvin and pressure is measured in atmospheres. This relation generalizes a large set of numerical simulations.

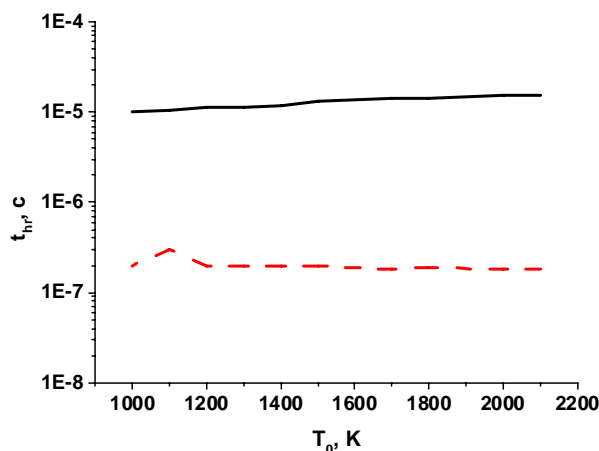


Figure 2a. Dependence of the heat release time on initial temperature of the self-igniting mixture. ——— - simulation,  $P_0 = 1$  atm,  $ER = 1$ ; - - - - simulation,  $P_0 = 15$  atm,  $ER = 1$ .

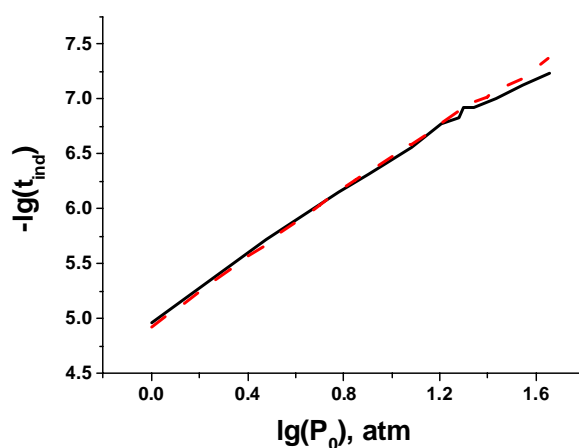


Figure 2b. Dependence of the heat release time on initial pressure of the self-igniting mixture. ——— - simulation,  $T_0 = 1200$  K,  $ER = 1$ ; - - - - simulation,  $T_0 = 1500$  K,  $ER = 1$ .

To interpret the results of the simulations, presented on Fig. 2, and to estimate the reaction order during the heat release the more extensive kinetic study of the hydrogen-air (oxygen) combustion was carried out. The range of conditions studied was: 1100 – 2100 K, 0.1 – 50 atm, equivalence ratio  $0.5 < ER < 3$ . It was found, that for the near-stoichiometric and rich conditions ( $0.8 < ER < 3$ ) in the temperature range 1100–2100 K and for the pressures 0.1–50 atm the peculiarities of the heat release stage are:

- 1) chain-propagation and chain-branching reactions are in quasi-equilibrium, while the time required for the transition to the quasi-equilibrium coincides with the time, required to attain the maximum heat release rate (usually accepted as induction time criterion);
- 2) concentrations for the species  $H_2O_2$ ,  $HO_2$ ,  $O$ ,  $OH$  are in quasi-steady-state;
- 3) concentration of the hydroxyl radical  $OH$  remains approximately constant while the heat release and is equal to the equilibrium concentration at adiabatic temperature of combustion;
- 4) rate-limiting stage of the heat release is the recombination reactions  $H + OH + M = H_2O + M$  with the zero activation energy and strong dependence on the pressure;
- 5) the recombination reaction  $H + OH + M = H_2O + M$  releases largest part of the chemical energy.

On the basis of the observed peculiarities it is possible to conclude that:

- 1) for the description of the heat release stage only one parameters is required thus justifying the IPM approach; in fact,

*number of independent parameters = number of total variables – number of auxiliary relations*,  
in our case *number of total variables* = 10 (temperature, eight mass fractions and density),  
*number of auxiliary relations* = 9 (2 conservations of the elements, conservation of energy,  
conservation of density, quasi-steady-state of the 4 species and quasi-equilibrium of one  
chain-propagation reaction), thus *number of independent variables* = 1.

- 2) the heat release rate practically does not depend on temperature as the activation energy of the recombination reaction  $H + OH + M = H_2O + M$  is zero, and the heat release rate very sensitive to pressure as the recombination reaction rate is very sensitive to pressure
- 3) the overall reaction order during the heat release stage is equal to 1 for the diluted mixtures of hydrogen and oxygen/air as the M concentration can be assumed constant and the OH concentration is constant as described above. For the undiluted mixtures this parameter should be selected more carefully by agreement of the ZND temperature profiles of the improved two-stage model and detailed kinetic simulations.

### 3 IMPROVED MODEL OF HYDROGEN DETONATIVE COMBUSTION: MODEL DESCRIPTION

To remove the difficulties of the original formulation of IPM model [5], three improvements are proposed. The first one is related with the introduction of the three effective species, which will replace the original set of species and two parameters  $f_i$  and  $f_{hr}$ , without increase in the number of differential equations. The second one is related with the tabulation of the induction time (from detailed kinetic simulations) and application of the newly developed economic algorithm for searching through the table instead of the calculation of the ignition delay times from analytical expressions, which are not accurate through the whole range of conditions. The third one is related with the changes in equation for the rate of heat-release stage.

Thus the improved model is stated as follows.

1) *Species*. The combustible mixture is composed of three species: A - reagent, B - intermediate and C - product,

$$\frac{1}{M_{a,b}} = \sum_i \frac{Y_{ir}}{M_i}, \quad H_{fa,b} = \sum_j Y_{rj} H_{fj}, \quad c_{pa,b}(T) = \sum_{i=0}^4 a_{a,bi} T^i, \quad a_{a,bi} = \sum_j Y_{rj} a_{ji},$$

$$\frac{1}{M_c} = \sum_j \frac{Y_{pj}}{M_j}, \quad H_{fc} = \sum_j Y_{pj} H_{fj}, \quad c_{pc}(T) = \sum_{i=0}^4 a_{ci} T^i, \quad a_{ci} = \sum_j Y_{pj} a_{ji},$$

$i$  is a component of the mixture (e.g., for hydrogen-oxygen mixtures with diluents  $i = \{H, O, OH, HO_2, H_2O_2, H_2O, H_2, O_2, N_2, Ar\}$ ),  $M_{a,b,c}$  – molar weight of the component A, B, C,  $a_{ja,b,c}$  –  $j$ -th coefficient in the polynomial approximation of the enthalpy and specific heat of the component A, B, C,  $a_{ji}$  –  $j$ -th coefficient in the polynomial approximation of the enthalpy and specific heat of the species  $i$ ,  $Y_{ir}$  – mass fraction of the  $i$ -th species in the initial mixture composition,  $M_i$  is their molar weights. The total heat of reaction is calculated at the pre-processor step

$$Q = \sum_i \frac{H_{fi}^0}{M_i} \cdot (Y_{ip} - Y_{ir})$$

where  $H_{fi}^0$  is heat of formation of the  $i$ -th species. The mass fraction  $Y_A$  of the reagent substance A is equivalent for  $f_i$  in original IPM model [5] ( $Y_A \equiv f_i$ ), the quantity  $1 - Y_B$  is equivalent for  $f_{hr}$  in original IPM model [5] ( $1 - Y_B \equiv f_{hr}$ ).

2) *Chemical kinetics*. The kinetic equations for the description of the combustion process and species transformations are

$$dY_a/dt = -\omega_a(Y_a, T, P), \quad dY_b/dt = -\omega_b(Y_a, Y_b, T, P)$$

a) *Induction stage description*.

During the induction stage the A component of the mixture is consumed: its mass fraction  $Y_A$  decreases from 1 to 0; at the same time the mass fraction of the B component increases from 0 up to 1 at the end of induction period.

To calculate the source terms in the kinetic equations, the dependence of the induction time on pressure and temperature is required in a wide range of pressures and temperatures:

$$\omega_a(Y_a, T, p) = \begin{cases} -\omega_i(T, p), & Y_a < 1, \\ 0, & Y_a = 1. \end{cases}$$

$$\omega_i(T, p) = t_{ind}^{-1}(T, p)$$

If the detailed chemical kinetic mechanism for the reactive mixture under consideration is known, than it is possible to calculate the induction times in a wide range of conditions and store them into the look-up table, which is loaded into the memory during the fluid dynamic simulation. In the current version of the IPM model the limits are settled to the following values:

- Minimum pressure is equal to initial pressure in the system;
- Maximum pressure is limited to  $10 \cdot P_{vN}$ , where the  $P_{vN}$  is von Neumann pressure of the steady 1D detonation wave;
- Minimum temperature is 900 K. If temperature is less than 900 K, than it is assumed that  $t_{ind}^{-1}(T, P) = 0$
- Maximum temperature is 2500 K. If the temperature is greater, than 2500 K, than the simple formula for induction time is used:

$$t_{ind}(T, P) = \frac{A}{P^\alpha}$$

as at high temperatures the ratio  $RT/E$  is not very small and induction time depends on temperature only slightly.

If the pressure  $P^*$  and temperature  $T^*$  at a given point of the flow do not strictly equal to values, stored in table, than the induction time is interpolated from the values in the vicinity of  $P^*$  and  $T^*$  according to the following algorithm:

- i. the values  $T_1$  and  $T_2$  are searched in the table and  $T_1 < T^* < T_2$ ;
- ii. the values  $P_1$  and  $P_2$  are searched in the table and  $P_1 < P^* < P_2$ ;
- iii. the values of the induction time  $t_{11} = t_{ind}(T_1, P_1)$ ,  $t_{12} = t_{ind}(T_1, P_2)$ ,  $t_{21} = t_{ind}(T_2, P_1)$ ,  $t_{22} = t_{ind}(T_2, P_2)$  are read from the look-up table;
- iv. the weighted Arrhenius-like interpolation [9, 12] is carried out

$$\tau = (1/T^* - 1/T_1)/(1/T_2 - 1/T_1), \quad \pi = (\ln(P^*) - \ln(P_1))/(\ln(P_2) - \ln(P_1))$$

$$\ln(t_{ind}(T^*, P^*)) = \ln(t_{11}) \cdot (1-\tau) \cdot (1-\pi) + \ln(t_{21}) \cdot \tau \cdot (1-\pi) + \ln(t_{12}) \cdot (1-\tau) \cdot \pi + \ln(t_{22}) \cdot \tau \cdot \pi.$$

As the dependence of the induction time on temperature and pressure exhibits Arrhenius-like characer (in general), than application of the Arrhenius-like approximation increases the accuracy of the interpolation and reduces the size of the look-up table. Usually, the table contains 15 – 17 point for temperature and 10 - 20 points for pressure, i.e. 150 – 340 point at all.

#### b) Heat-release stage

The heat release stage is described by the change in the concentration of the B species (intermediates):

$$\omega_b(Y_a, Y_b, T, p) = \begin{cases} \omega_i(T, p), & Y_a < 1, \\ -\omega_{hr}(Y_b, T, p), & Y_a = 1. \end{cases} \quad \omega_{hr}(Y_b, T, P) = a \left( \frac{P}{P^*} \right)^{np} \left( \frac{T}{T^*} \right)^{nt} Y_b^{nf} \exp\left(-\frac{b}{T}\right)$$

To account for the strong dependence of the heat release rate on pressure and temperature and to generalize the model parameters (to avoid the new calculation of the parameters for another initial conditions), the following modification of the heat-release stage is proposed on the basis of the simulation results, presented in the section 2:

$$\omega_{hr}(Y_B, T, P) = a \left( \frac{P}{P^*} \right)^{np} \left( \frac{T}{T^*} \right)^{nt} Y_B^{nf} \exp\left(-\frac{b}{T}\right),$$

where the  $P^*$  and  $T^*$  are pressure and temperature, at which the parameters of the model are evaluated and  $ER$  is equivalence ratio of the mixture.

Pre-exponential factor is defined according to the relation

$$a = \frac{1}{t_{hr}(T^*, P^*, ER)},$$

where the heat release time  $t_{hr}(T^*, P^*, ER)$  is calculated on the basis of the kinetic simulations with the detailed kinetic mechanism.

Reaction order relative to pressure is determined from the relation

$$n_p = -\frac{\partial \ln[t_{hr}(T^*, P^*, ER)]}{\partial \ln P^*},$$

and for hydrogen-air mixtures it is equal to  $n_p = 1,5$ .

Reaction order relative to progress variable  $Y_B$  must be found from kinetic considerations and for hydrogen-air mixtures

$$n_f = 1,$$

according to section 2.

Activation energy  $b$  and parameter  $n_T$  are defined from relation

$$n_T + \frac{b}{T^*} = -\frac{\partial \ln[t_{hr}(T^*, P^*, ER)]}{\partial \ln T^*}.$$

#### 4 EXAMPLE: HYDROGEN-OXYGEN MIXTURES

As example, the stoichiometric hydrogen-air and hydrogen-oxygen mixtures at pressure 1 atmosphere and temperature 300K will be considered. All the kinetic calculations are carried out in the Chemical Workbench<sup>®</sup> software suite [10], and the Marinov's kinetic mechanism [11] was used.

##### a) Induction stage parameters

The boundaries for the look-up table of induction times are:

$$P_{min} = 1 \text{ atm}; P_{max} = 330 \text{ atm for hydrogen-oxygen}; P_{max} = 270 \text{ atm for hydrogen-air};$$

$$T_{min} = 900\text{K}; T_{max} = 2500\text{K}.$$

For the temperatures, higher than 2500 K the approximation

$$t_{ind}(T, P) = 1.33 \cdot 10^{-6} \cdot \left(\frac{1}{P}\right)^{0.96} \text{ for H}_2\text{-air and } t_{ind}(T, P) = 5.77 \cdot 10^{-7} \cdot \left(\frac{1}{P}\right)^{0.96} \text{ for H}_2\text{-O}_2.$$

##### b) Heat-release stage parameters

For hydrogen-air mixture the following parameters for the heat-release stage are ( $T^* = 1100$  K and  $P^* = 1$  atm):  $a = 4,34 \cdot 10^4 \text{ s}^{-1}$ ,  $n_p = 1,5$ ,  $n_f = 1$ ,  $b = 0$  K.

The similar approach could be applied for hydrogen-oxygen mixtures and the heat-release parameters for this mixture are:  $a = 1,7 \cdot 10^5 \text{ s}^{-1}$ ,  $n_p = 1,5$ ,  $n_T = 0$ ,  $n_f = 1$ ,  $b = 0$  K

##### c) ZND structure of the steady detonation wave in hydrogen-oxygen mixtures

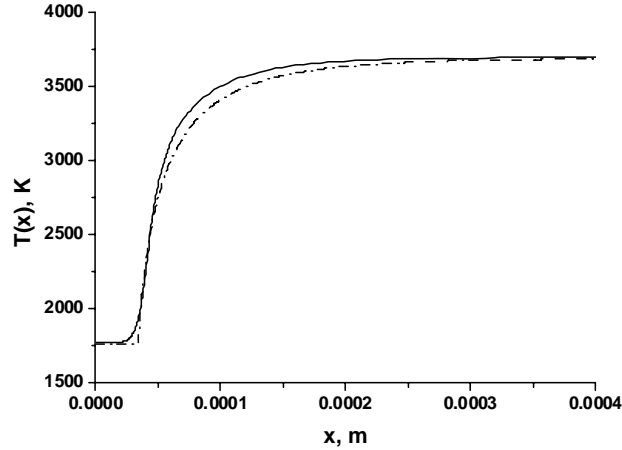


Figure 3. ZND structure of the steady detonation wave in stoichiometric  $H_2/O_2$  mixture at initial temperature 300 K and pressure 1 atm. ——— - simulation, detailed chemical kinetic mechanism [11]; - - - - simulation, modified IPM model.

The temperature profile in the ZND structure of a detonation wave in stoichiometric  $H_2/O_2$  mixture is plotted at the Fig. 3. Initial temperature  $T_0 = 300$  K and pressure  $P_0 = 1$  atm, Chapman-Jouguet speed of the detonation wave is  $D_{CJ} = 2842$  m/s. Parameters of the gas just behind the leading shock front of the detonation wave  $T_{vN} = 1770$  K,  $P_{vN} = 33$  atm. The solid curve at the Fig. 3 is the temperature profile, obtained with the detailed kinetic mechanism [14] using the ZND model, implemented in the Chemical Workbench software [13]. The dashed line is the same ZND profile, obtained using the modified IPM model with the parameters  $a = 1,7 \cdot 10^5$  s<sup>-1</sup>,  $n_p = 1,5$ ,  $n_T = 0$ ,  $n_f = 1$ ,  $b = 0$  K. In spite of the fact, that the reference pressure and temperature  $T^* = 1100$  K and  $P^* = 1$  atm are far enough from the von Neumann conditions, the ZND structure of the detonation wave is reproduced accurately.

## 5 CELLULAR STRUCTURE OF THE TWO-DIMENSIONAL DETONATION WAVE

### 1) Problem formulation

Initiation of the 2D detonation wave, propagating in the channel 1m long and 6 or 8 cm height is performed as in the previous work, devoted to simulation of the cellular structure with the detailed chemical kinetic mechanism [13]. The mixture under consideration is  $H_2:O_2:Ar = 2:1:7$  at temperature 300 K and pressure 6670 Pa.

The ZND structure of the detonation wave, propagating from left to the right was re-interpolated on 2D mesh, its front is placed on the distance of 8 cm from the left boundary of computational domain (see figures below). The disturbance is introduced into the flow by 3 mm behind the leading front of the detonation wave, its length along the direction of the detonation propagation is 1 cm, its size in the orthogonal direction is 1.4 cm, the disturbance in symmetric relative to central line of the 2D channel. The pressure and temperature in the undisturbed region is 7 times higher than initial conditions ahead of the detonation wave front.

The ZND induction length of the steady detonation wave in  $H_2:O_2:Ar = 2:1:7$  mixture at initial pressure 6670 Pa and temperature 300 K is equal to 1.2 mm. In [5] the convergence study was performed, which showed, that in the simulations with the detailed chemical kinetic mechanism [13] the convergence of the simulations was attained, if the size of the computational cell was equal or less, than  $1,5 \cdot 10^{-4}$  m in the direction of the wave propagation. In the present work the convergence study for the new IPM model was performed for new flow solver [15]. The comparison of the maximum pressure behavior at the center line of the channel has shown that the convergence was attained for the computational cell size  $3 \cdot 10^{-4}$  m. All the simulations, presented below, are carried out with the cell size  $3 \cdot 10^{-4}$  m.



## 2) Simulation of the cell size of the detonation and comparison with the detailed chemical kinetic mechanism predictions

To test the predictive capabilities of the proposed improved IPM model, the 2D cellular structure of the detonation wave was simulated and compared with the results of the simulations with the detailed kinetic mechanism (parameters of the model were calculated with the same mechanism). The calculation was performed in the channel of 6 cm height and 1 m long.

Parameters of the model were calculated at:  $P^* = 101325$  Pa,  $T^* = 1500$  K, and were equal to  $a = 7.4 \cdot 10^4$  s<sup>-1</sup>,  $b = 0$  K,  $n_p = 1.72$ ,  $n_t = 0$ ,  $n_f = 1$ .

In the channel of the 6 cm height the cellular structure with two cells across the channel is formed, see Fig. 4a (upper half of the channel is shown), i.e. the cell size is equal to 3 cm, the cell size along the channel axis is 5.1 cm, its ratio is 0.59. The picture of the foot-prints is regular and steady during the long period of time up to the moment, when the detonation wave reaches the right boundary of the channel. In [16] the simulation of the detonation cell size in the same mixture and at the same conditions was carried out with the detailed chemical kinetic mechanism [13]. It was shown, that the cell size across the channel is 3 cm as well, but the cell size along the channel was 5.5 cm, ratio of the cell size across and along the channel is 0.55. The calculated history of the wave propagation with the detailed chemical kinetic mechanism [13] is given on the Fig. 6b. Comparison of the Figs. 4a and 4b shows, that an overall sequence of the formation of the gas dynamic disturbance, interaction of the compression waves and shock waves, formation of the cellular structure is very similar in both types of the simulations (with improved IPM and detailed chemical kinetic mechanism [13], [16]).

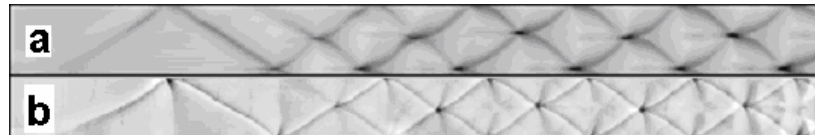


Figure 4. a) Formation of the cellular structure of the detonation wave, simulated with improved IPM model (current paper), б) the same, but with detailed chemical kinetic mechanism, extracted from [13]. Only the upper part of the channel is shown.

To determine the bottom and upper boundaries of the cell size for the mixture and conditions under consideration, the additional set of simulations was performed for the channel heights 6 cm, 8 cm, 9 cm and 12 cm. The series of the calculation has shown, that the estimation for the cell size of the mixture and conditions under consideration is

$$3 \text{ cm} < \lambda < 4 \text{ cm}.$$

## 3) Influence of the heat release order to pressure on the results of the simulations

It is obvious, that the change in the parameter  $a$  of the modified IPM model will result in the change of the cell size of the detonation wave, as the length of the heat release zone will change respectively.

But the change of the parameters  $n_p$  and  $n_f$  is not so clear. Actually, even if the parameters  $n_p$  and  $n_f$  are changed, the heat release rate after the completion of the induction stage is the same for all the cases and equal to  $a \cdot Q$ . The change of  $n_p$  and  $n_f$  results only to small change in the structure of the detonation wave. The question under consideration is important, because in the original version of the IPM mode [5]  $n_p = 0$ ,  $n_f = 1$ , but in the another type of the two-stage models, developed by Yu.N. Nikolaev [6],  $n_f = 2$ . In the present section the influence of the  $n_p$  parameter value on the results of the predictions of the cell size is investigated.

First, the change of the heat release zone in the steady detonation wave is investigated for different values of  $n_p$ . For this purpose the steady ZND structure of the detonation wave, propagating with Chapman-Jouguet speed was simulated with the improved version of the IPM model. To keep the heat release rate independent on  $n_p$  value, the parameters of the model were calculated at von Neumann conditions,  $P_{vN} = 1.72$  atm,  $T_{vN} = 1860$  K,  $P^* = P_{vN}$ ,  $T^* = T_{vN}$  and were equal  $a = 7.4 \cdot 10^4$  s<sup>-1</sup>,  $b = 0$  K,  $n_p = 1.72$ ,  $n_t = 0$ ,  $n_f = 1$ .

The results of the simulations show, that the change of  $n_p$  does not results into the change of the steady detonation wave structure and the major part of the heat is released through the 3 mm of the

heat release zone of the detonation wave. The value of the  $n_p$  determines only the distance, where the Chapman-Jouguet condition will be satisfied. Therefore, the influence of the  $n_p$  on the structure of the steady detonation wave is weak (for the explored range  $0 \leq n_p \leq 3$ ).

To understand the role of  $n_p$  in the formation of the cellular structure of the detonation wave, the series of the 2D simulations was carried out in the channels with the height 6 cm and 8 cm. The results are presented on the Fig. 5 (channel height 6 cm) and Fig. 6 (channel height 8 cm).

The presented figures allow to draw a conclusion, that the influence of the parameter  $n_p$  on the formation of the cellular structure is strong. If the dependence of the heat release rate on pressure is not included into calculation, than it is impossible to get the results, which are in agreement with the simulations with the detailed chemical kinetic mechanism.

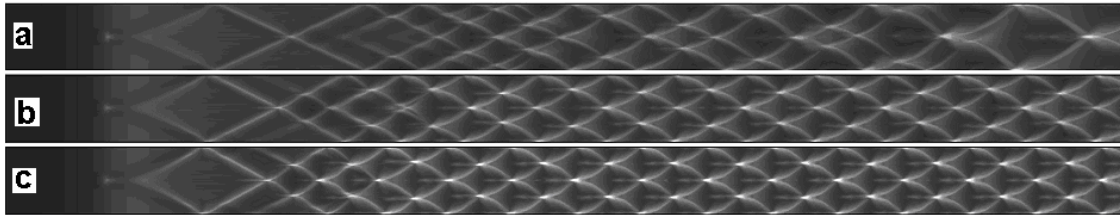


Figure 5. Formation of the cellular structure of the detonation wave in the channel 6 cm height. a –  $n_p = 0$ , b –  $n_p = 1$ , c –  $n_p = 1.72$ .

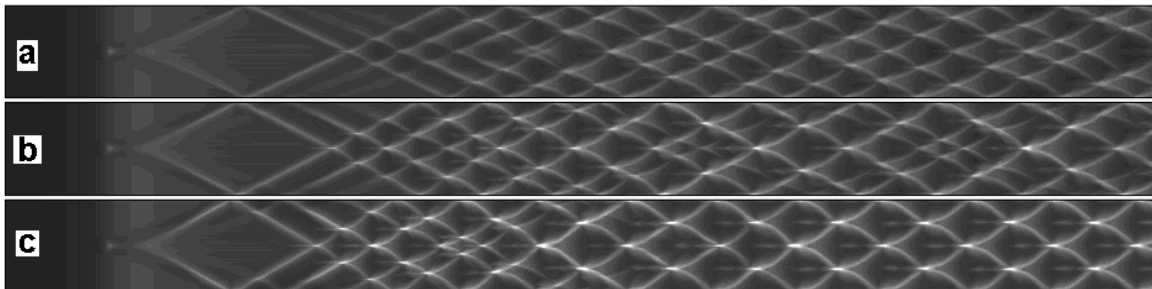


Figure 6. Formation of the cellular structure of the detonation wave in the channel 8 cm height. a –  $n_p = 0$ , b –  $n_p = 1$ , c –  $n_p = 1.72$ .

Comparison of the results of the simulations with the different channel heights and different  $n_p$  shows that increase of the sensitivity of the heat release to pressure has a stabilizing effect on the formation of the cellular structure and transition to stationary regime occurs faster. For example, in the channel with the height 6 cm for  $n_p = 0$  only one cell is formed per channel height. The transition to this regime requires distance of 0.8 m. If  $n_p = 1$ , than two cells are formed per channel height, but some irregularity is present in the formed pattern, the cell size in the central part of the channel periodically changes. To form the final pattern, the distance of 0.36 m is required. Regular picture is formed for  $n_p = 1.72$ , the formation of the stationary pattern is observed on the distance of 0.28 m.

In the channel with the height 8 cm the observed pattern becomes more irregular, than for 6 cm channel. In the simulation with  $n_p = 0$  the transition to the stationary pattern is not observed for 1 m length. Probably, the increase of the computational domain results in the stationary pattern with 1 cell per channel height, that is justified by the calculations with another values of  $n_p$ , where the steady regime coincided with that, observed in the channel 6 cm height.

Stabilizing effect of the heat release dependence on pressure is explained by the increased non-linearity of the evolution of the transverse disturbances: among several weak waves the strongest will increase faster, another disturbances will gradually decreases and disappear. If  $n_p = 0$ , all disturbances are equivalent and remain in the pattern for a long time (see Figs. 5a and 6a).

Thus, allowing for the dependence of the heat release rate on pressure is important and should be taken into consideration for two reasons.

#### 4) Influence of the heat release reaction order on the results of the simulations

In this section the influence of the parameter  $n_f$  on the cellular pattern of the detonation wave is investigated.

Firstly, the change of the structure of the steady detonation wave with  $n_f$  was investigated. The speed of the detonation wave was Chapman-Jouguet speed, 1618 m/s. Coefficients of the model were calculated at von Neumann conditions,  $P_{vN} = 1.72$  atm,  $T_{vN} = 1860$  K,  $P^* = P_{vN}$ ,  $T^* = T_{vN}$  and were equal  $a = 7.4 \cdot 10^4$  s<sup>-1</sup>,  $b = 0$  K,  $n_p = 1.72$ ,  $n_t = 0$ .

The results of the simulations of the ZND structure of the detonation wave have shown, that that some change of the structure of the detonation wave is observed: the amount of energy, released on a certain distance decreases with the increase of  $n_f$ , and increase of  $n_f$  shifts the point, where the Chapman-Jouguet condition is attained very far from the leading shock of the detonation wave. Note, that for  $n_f < 1$  the length of the reaction zone is finite, e.g. for  $n_f = 0,5$  the sum of induction length and reaction length is 0.0145 m. For  $n_f \geq 1$  the length of the reaction zone is infinite, e.g. for  $n_f = 1$  local Mach number 0.971 is attained only on the distance 8 cm behind the leading shock front.

Thus, the change of the reaction order results in redistribution of the intensity of the heat release in the reaction zone and shifts the Chapman-Jouguet plane far from the leading shock.

To understand the role of the parameter  $n_f$  in the formation of the steady structure of the cellular pattern, the set of simulations was carried out for the channels with the height 6 cm and 8 cm. Results of the simulations are presented on the Fig. 7 (channel height 6 cm) and Fig. 8 (channel height 8 cm). The simulations were carried out for  $n_f = 0$ ,  $n_f = 1$ ,  $n_f = 2$ .

Results of the simulations for the channel height 6 cm show, that the cell size is strongly dependent on value of  $n_f$ . For the simulations with  $n_f = 0$  and  $n_f = 1$ , the regime with two cells per channel height lasts for a long time, but after some time in the simulation with  $n_f = 0$  the cellular pattern becomes irregular and transits to the regime with one cell per channel height. It is worth pointing out the increased pressure in the points of the collision of the transverse waves. This observation can be explained by short reaction zone in this case.

In the simulation with  $n_f = 2$  the pattern with one cell per channel height forms on the distance of 0.37 m. Probably, the observed result is explained by the redistribution of the heat release and influence of the rarefaction wave. In this case it is preferable to propagate in the regime with one cell and high pressure in the collision points.

Simulations for the channel with 8 cm height shows, that the value of  $n_f$  is important as well. Depending on the value of  $n_f$  the different number of cells per channel height is observed. It is interesting to note, that the number of cells is the same for both channels (6 cm and 8 cm) in the case with  $n_f = 1$ .

Thus, change of the reaction order on the heat release stage results in the re-distribution of the heat release and influences the process of cellular pattern formation and its final view.

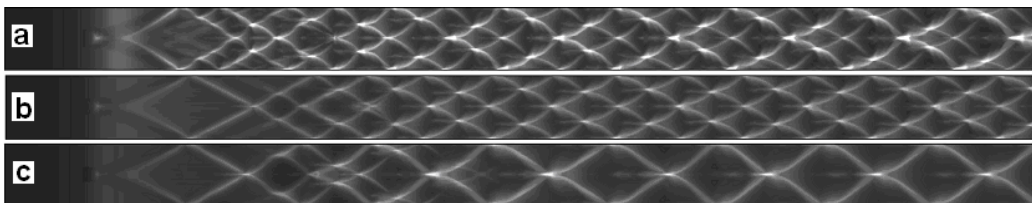


Figure 7. Formation of the cellular pattern of the detonation wave in the channel with 6 cm height. a –  $n_f = 0$ , b –  $n_f = 1$ , c –  $n_f = 2$ .

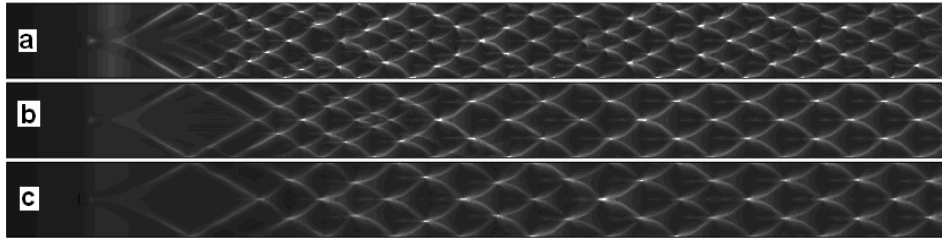


Figure 8. Formation of the cellular pattern of the detonation wave in the channel with 8 cm height. a –  $n_f = 0$ , b –  $n_f = 1$ , c –  $n_f = 2$ .

## 6 CONCLUSIONS

In the present paper the improved induction parameter model (IPM) for hydrogen is described in details. The main improvements are:

- look-up tables for the induction times, stored in the memory and algorithm for induction time calculation from these tables;
- description of the reactive mixture composition by three species, which thermodynamic properties are calculated on the basis of the properties of the real reagents and products;
- improvement of the heat release stage description according to the main kinetic features, observed in the simulations with the detailed kinetic mechanism: sensitivity to the pressure and calculation of the parameters of the model from the pure kinetic simulation without fluid dynamics simulations.

In the series of the 2D fluid dynamic simulations it was demonstrated, that the proposed improvements to IPM model are important, as the particular values of the model parameters are important in the evaluation of the cell size of the detonation wave (and other dynamic parameters of the detonation as consequence). The parameter values, calculated with the improved model allow to get the results, which are consistent with the detailed kinetic mechanism, thus the proposed improvements are important.

## REFERENCES

1. W. Fickett and W. Davis. Detonation. Dover Publications, 1979.
2. Korobeinikov V.P., Problems of Point-blast theory, American Institute of Physics, 1991
3. Oran, E. S., Jones, D. A. & Sichel, M. 1992. *Proc. R. Soc. Lond.* A436, 267 - 297.
4. Lefebvre, M.H., Oran, E.S., , *Shock waves*, vol. 4, 277-283.
5. M. Sichel, N.A. Tonello, E.S. Oran, D.A. Jones., *Proc. R. Soc. Lond. A*, vol. 458, 49-82
6. Nikolaev, Yu.A., *Fizika Goreniya I vzriva*, 1978. vol. 14, No. 5, P. 73
7. Trotsyuk, A.V., *Combustion Explosion Shock waves*, vol. 35, No. 5, 549-558
8. B. Varatharajan, M. Petrova, F. A. Williams, and V. Tangirala. In *Proceedings of the Combustion Institute*, volume 30, pages 1869–1877, 2005.
9. Eckett C.A. (2001),. Ph.D. thesis, University of California, Pasadena <http://galcit.caltech.edu/EDL>
10. M. Deminsky, V. Chorkov, G. Belov, I. Cheshigin, A. Knizhnik, E. Shulakova, M. Shulakov, I. Iskandarova, V. Alexandrov, A. Petrushev, I. Kirillov, M. Strelkova, S. Umanski, B. Potapkin. *Computational Materials Science*, 2003, vol. 28, p. 169—178
11. Marinov, N. M., Westbrook, C. K., and Pitz, W. J., in *Eighth (International) Symposium on Transport Processes*, vol. 1, 1995, pp. 118–129
12. Gregory P. Smith, David M. Golden, Michael Frenklach, Nigel W. Moriarty, Boris Eiteneer, Mikhail Goldenberg, C. Thomas Bowman, Ronald K. Hanson, Soonho Song, William C. Gardiner, Jr., Vitali V. Lissianski, and Zhiwei Qin [http://www.me.berkeley.edu/gri\\_mech](http://www.me.berkeley.edu/gri_mech)
13. Oran E.S. and Boris J.P., *Combustion and Flame*, 48: 149-161, (1982)
14. Oran E. S., Weber J. E., Stefaniw E. I., Lefebvre M. H. and Anderson J. D., *Combustion and Flame*, Vol. 113, pp. 147–63
15. I.A. Kirillov, E.V. Osinina, A.V. Panasenkov, M.I. Strelkova, *Mathematical modeling*, V. 17, No. 11, p. 93, 2005 (in Russian)
16. R. Deiterding, PhD thesis, Brandenburgische Technische Universität Cottbus, Sep 2003, 280 p.